New Low-Dimensional Quaternary Sulfides $NaCuMS_2$ (M = Mn, Fe, Co, and Zn) with the $CaAl_2Si_2$-Type Structure: Synthesis and Properties

M. Oledzka, K. V. Ramanujachary,† and M. Greenblatt*

Chemistry Department, Rutgers, The State University of New Jersey, P.O. Box 939, Piscataway, New Jersey 08855-0939

Received July 8, 1997. Revised Manuscript Received November 7, 1997

The synthesis, structure, and electronic properties of a series of new quaternary layered sulfides, $NaCuMS_2$ (M = Mn, Fe, Co, Zn) are reported. The synthesis was accomplished by sulfurization of a mixture of oxide or sulfide and carbonate precursors of the corresponding metals by nitrogen gas charged with CS_2. All of the phases crystallize in the trigonal $CaAl_2Si_2$-type structure in space group $P\bar{3}m1$. The electrical resistivity measurements show that all of the new phases are semiconducting, with room-temperature resistivities ρ_{RT} varying from 6.2×10^{-1} to 5×10^{-2} Ω·cm, depending upon the transition metal M. The magnetic susceptibility measurements indicate the presence of localized Mn^{2+} ions in $NaCuMnS_2$. The $NaCuMS_2$ (M = Fe, Co) phases display temperature-independent paramagnetism, whereas the $NaCuZnS_2$ phase is diamagnetic as expected. In addition, detailed low-temperature magnetic studies of the $NaCuFeS_2$ phase revealed spin-glass-type behavior with the freezing temperature $T_f \sim 50$ K.

Introduction

Layered quaternary sulfides that form upon alkali ion insertion into the chalcopyrite, $CuFeS_2$, have attracted attention as potential candidates for intercalation cathodes. In particular, $LiCuFeS_2$ has been considered as a cathode material for applications in high-temperature secondary lithium batteries.[1] Insertion of alkali metal ions into the three-dimensional (3D) framework of the chalcopyrite (Figure 1a) leads to the formation of new layered quaternary sulfides with the formula $ACuFeS_2$ (A = Li, Na, K, Rb, Cs).[1−5] Interestingly, depending on the size of the intercalating alkali ion, *A*, two different crystallographic structures have been reported. This difference in the structures is also manifested in the naturally occurring minerals, *chvilevait* Na(Cu, Fe, $Zn)_2S_2$[6] and *murunskite* $K_2Cu_3FeS_4$ ($KCu_{1.5}Fe_{0.5}S_2$).[7] The insertion of a smaller alkali metal ion, such as Li^+ or Na^+, results in the trigonal $CaAl_2Si_2$-type structure similar to $LiCuFeS_2$ (Figure 1b). This structure is characterized by the hexagonal closed packing of the sulfur anions with the copper and iron ions in the tetrahedral holes. The alkali ions occupy the octahedral holes in the van der Waals gap.[8,9] On the other hand, insertion of larger cations such as K^+, Rb^+, or Cs^+ leads to the well-known $ThCr_2Si_2$-type structure. As illustrated in Figure 1c, in this type of structure, layers of edge-sharing sulfur tetrahedra with the copper and iron ions in the centers are extended in the *ab* plane. The alkali metal ions occupy the 8-fold coordinated site formed by sulfide ions.[10]

Apart from the structural differences noted above, contrasting differences in the electrical and magnetic properties are also observed upon alkali ion intercalation. For example, the long-range magnetic order (LRMO) observed in the chalcopyrite is lost upon alkali ion intercalation.[1−5] The absence of LRMO in the $ACuFeS_2$ phases has been rationalized on the basis of the random distribution of Cu and Fe ions at the tetrahedral site, as suggested by the single-crystal X-ray diffraction studies.[1−5] However, X-ray diffraction does not provide unambiguous resolution on the question of order/disorder of Cu and Fe, because of the similarity of the X-ray scattering power of Cu and Fe. Neutron diffraction studies might provide a definite proof. Recently, Ramírez et al. have examined the possibility of transition metal ions ordering in the $ACuFeS_2$ (A = Li, Na) phases by band structure calculations and Monte Carlo simulations.[11] According to their calculations, the formation of Fe−Fe pairs is energetically more favorable

* To whom correspondence should be addressed.
† Current address: Rowan University of New Jersey, Department of Chemistry, Glassboro, NJ 08828.

(1) Fong, R.; Dahn, J. R.; Batchelor, R. J.; Einstein, F. W. B.; Jones, C. H. W. *Phys. Rev. B* **1989**, *39*, 4424.
(2) Llanos, J.; Contreras-Ortega, C.; Mujica, C. *Mater. Res. Bull.* **1993**, *28*, 39.
(3) Mujica, C.; Paez, J.; Llanos, J. *Mater. Res. Bull.* **1994**, *29*, 263.
(4) Mujica, C.; Llanos, J.; Guzmán, M.; Contreras-Ortega, C. *Nucleotecnica* **1994**, *14*, 23.
(5) Llanos, J.; Valenzuela, P.; Mujica, C.; Buljan, A.; Ramirez, R. *J. Solid State Chem.* **1996**, *122*, 31.
(6) Katchalovskaya, W. M.; Osipov, B. S.; Nazarenko, N. G.; Kykoyev, W. A.; Mazmanian, A. O.; Yegorov, I, N.; Kaplunnik, L. N. *Zap. Vses. Mineral. O-va* **1988**, *117*, 204.
(7) Dobrovolskaya, M.; Rogova, W. P.; Celin, A. I.; Malov, W. *Zap. Vses. Mineral. O-va* **1980**, *110*, 468.
(8) (a) Gladysevskij, E. I.; Kripjakevic, P. I.; Bodack, O. I. *Ukr. Fiz. Zh.* **1967**, *12*, 447. (b) *Structure Reports*; Pearson, W. B., Ed.; Oosthoek, Scheltema, & Holkema: Utrecht; 1975; Vol. 32A, p 5.
(9) Batchelor, R. J.; Einstein, F. W. B.; Jones, C. H. W.; Fong, R.; Dahn, J. R. *Phys. Rev. B* **1988**, *37*, 3699.
(10) Ban, Z.; Sikirica, M. *Acta Crystallogr.* **1965**, *18*, 594.
(11) Ramírez, R.; Buljan, A.; Noya, J. C.; Llanos, J. *Chem. Phys.* **1994**, *189*, 585.

S0897-4756(97)00479-1 CCC: $15.00
Published on Web 01/19/1998

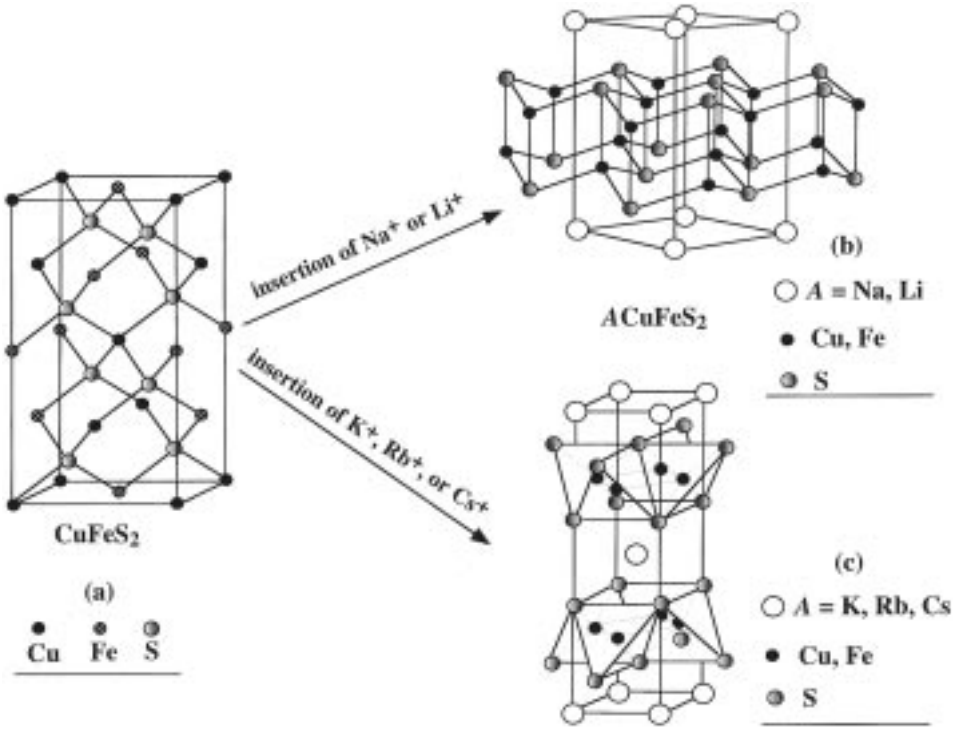

Figure 1. Unit cell of (a) chalcopyrite $CuFeS_2$, (b) $ACuFeS_2$ (A = Li, Na) with the $CaAl_2Si_2$-type structure, (c) $ACuFeS_2$ (A = K, Rb, Cs) with the $ThCr_2Si_2$-type structure.

and hence affects the distribution of the iron and copper ions in the $LiCuFeS_2$ and $NaCuFeS_2$ phases. This pairing, in turn, should lead to an observable short-range magnetic order (SRMO) in both phases.

As part of our work on the quaternary sulfide systems with the formula $ACuMS_2$ (A = alkali metal; M = 3d transition metal), we have recently reported on the transport properties of $ACuFeS_2$ (A = K, Rb, Cs) compounds.[12] In the course of this investigation, we have also synthesized a series of novel quaternary sulfides $ACuMS_2$ (A = K, Rb, Cs; M = Mn, Co)[13,14] with $ThCr_2Si_2$-type of structure. The formation of $ACuMS_2$ (A = K, Rb, Cs; M = Mn, Co, Fe) phases and that of the $NaCuFeS_2$ phase suggests that the replacement of iron in $NaCuFeS_2$ by either Mn or Co should lead to new compounds, $NaCuMnS_2$ and $NaCuCoS_2$. Moreover, the report on the mineral chvilevait with the formula $Na(Cu, Fe, Zn)_2S_2$ by Katchalowskaya et al.[6] suggested the possible existence of a new quaternary sulfide, $NaCuZnS_2$. In fact, the crystal structures of cubic ZnS (zinc blende) and the chalcopyrite $CuFeS_2$ are related; the latter is a superstructure of zinc blende by replacement of Zn by equal numbers of Cu and Fe atoms.[15] The ordering of Cu and Fe at the cation sites of zinc blende results in an approximate doubling of the *a*-axis, leading to the tetragonal chalcopyrite structure. Furthermore, "$CuZnS_2$" with the chalcopyrite structure is not known. This is to be expected, since copper is monovalent in the chalcogenides,[16] and this would require Zn to be in the improbable trivalent state. Although metastable β-MnS is also known to adopt the zinc blende-type structure, the corresponding sulfides of iron, cobalt or copper do not adopt this structural type.[17] The ternary "$CuMnS_2$" and "$CuCoS_2$" phases have not been reported as yet. To our knowledge, the only reported ternary phases in such mixed-transition metal sulfide systems are: (1) the metallic spinel $CuCo_2S_4$,[18] and its derivatives with various transition metal contents (e.g., superconducting $Cu_{1.5}Co_{1.5}S_4$[19]), and (2) the metallic mixed-transition metal pyrites $Mn_yCu_{1-y}S_2$ ($y \approx 0.01-0.8$).[20]

In this paper we report the synthesis and physical properties of a series of new low-dimensional sulfides, $NaCuMS_2$ (M = Mn, Fe, Co, Zn). All of the compounds were prepared by the CS_2/N_2 sulfurization method. The ternary compounds $NaMM'S_2$ (M or M′ = Mn, Fe, Co, Cu, Zn) with $CaAl_2Si_2$-type structure have not been reported to date. Therefore, the novel $NaCuMS_2$ phases (M = Mn, Fe, Co, Zn), described in this work, represent the first examples of such quaternary compounds in the growing family of Cu-containing multinary chalcogenides.[21]

Experimental Section

Synthesis. $NaCuCoS_2$ was synthesized by sulfurization of the precursor mixture containing Na_2CO_3 (Aldrich 99.95%),

(12) Oledzka, M.; Ramanujachary, K. V.; Greenblatt, M. *Mater. Res. Bull.* **1996**, *31*, 1491.
(13) Oledzka, M.; Lee, J.-G.; Ramanujachary, K. V.; Greenblatt, M. *J. Solid State Chem.* **1996**, *127*, 151.
(14) Oledzka, M.; Lee, C. L.; Ramanujachary, K. V.; Greenblatt, M. *Mater. Res. Bull.* **1997**, *32*, 889.
(15) Wells, A. F. *Structural Inorganic Chemistry*; Clarendon Press: Oxford, 1975; p 631.
(16) Folmer, J. C. W.; Jellinek, F. *J. Less-Common Met.* **1980**, *76*, 153.
(17) Rao, C. N. R.; Pisharody, K. P. R. *Prog. Solid State Chem.* **1976**, *10* (4), 207.
(18) Jellinek, F. *MTP International Review of Science, Inorganic Chemistry Series I*; Butterworth: London, 1972; p 339.
(19) Furukawa, Y.; Wada, S.; Miyatani, K.; Tanaka, T.; Fukugauchi, M.; Ishikawa, M. *Phys. Rev. B: Condens. Matter* **1995**, *51*, 6159.
(20) Bither, T. A.; Donohue, P. C.; Cloud, W. H.; Bierstedt, P. E.; Young, H. S. *J. Solid State Chem.* **1970**, *1*, 526.
(21) Keane, P. M.; Lu, Y. L.; J. A. Ibers, J. A. *Acc. Chem. Res* **1991**, *24*, 223.

Co_3O_4 (Alfa Aesar, 99.9985%), and CuO (Alfa Aesar 99.9%). The starting materials were mixed in a ratio 3/2:2/3:2 respectively, ground thoroughly, and pressed into a pellet (10 000 psi). A slight excess of sodium carbonate was observed to facilitate the formation of well-crystallized single phases. The pellet was placed in an alumina boat in a tube furnace in a stream of dried nitrogen charged with carbon disulfide, CS_2. After being heated to ~1100 K and kept at this temperature for 12 h, the furnace was shut off and allowed to cool to room temperature at a rate of approximately 100°/h in the N_2 flow. The cooled melt was then extracted mechanically from the boat and dissolved in water under inert atmosphere to remove the sodium polysulfides. The shiny silver polycrystalline material that remained was washed and dried with anhydrous ethyl ether. $NaCuCoS_2$ crystallizes in the form of very thin mica-like sheets, which are stacked one on top of another. $NaCuCoS_2$ is stable, if stored under water, but oxidizes rapidly in air. Consequently, all measurements were made on samples, which had been stored in a drybox.

The compounds $NaCuMnS_2$, $NaCuFeS_2$, and $NaCuZnS_2$ were prepared in a similar manner by sulfurizing a mixture made up of Na_2CO_3, CuO, and either MnS (Alfa Aesar 99.9% pure) or Fe_2O_3 (Johnson Matthey 99.9% pure) or ZnO (Alfa 99.9% pure) in a 3/2:2:2 ratio. The $NaCuFeS_2$ phase forms as a polycrystalline material with a golden metallic luster. The reactivity of $NaCuFeS_2$ toward air and moisture seems to depend on the degree of crystallization; larger crystals are moderately stable in water and air whereas fine powder samples decompose immediately upon exposure to either. The $Li_{2.3}CuFeS_2$ phase, which is isostructural with $NaCuFeS_2$, was reported to exhibit similar behavior.[22] In contrast to the $NaCuCoS_2$ and $NaCuFeS_2$ phases, the $NaCuMnS_2$ and $NaCuZnS_2$ compounds are stable in air. Upon grinding, the $NaCuMnS_2$ phase becomes light-brown and the $NaCuZnS_2$ phase becomes bright-yellow.

Characterization. Powder X-ray diffraction (PXD) profiles, collected with an automated SCINTAG PAD V diffractometer and CuKα radiation, were used to confirm the monophasic nature of the samples. The lattice parameters were refined by a least-squares program, fitting over the 2θ range 10−60°, with KCl powder as an internal standard. The slides for the X-ray diffraction measurements of air-sensitive phases, $NaCuMS_2$ (M = Fe, Co), were prepared in a drybox, and the sample was protected by a polyethylene foil. Prior to the transport measurements, the powder samples were pressed into pellets and sintered at ~900 K in nitrogen atmosphere charged with CS_2. Elemental analyses of the compounds were done by JEOL JXA-8600 superprobe, by Amray 1400 Scanning Electron Microscope (SEM) equipped with an energy-dispersal X-ray (EDS) analysis facility, and by direct current plasma atomic spectrometric (DCP-AES) method with sodium, manganese, iron, cobalt, copper, and zinc AA/ICP calibration/check standards for environmental analysis (purchased from Aldrich). The dc resistivity measurements were carried out by a standard four-probe technique with a closed-cycle cryostat (APD Cryogenics, DE 202) from room temperature down to ~30 K. Ohmic contacts were made by attaching molten indium ultrasonically to four spots of a brick-shaped polycrystalline pellet in a stream of N_2 gas. The uncertainty in the resisitivity measurement is about 15%. Qualitative Seebeck measurements were performed to determine the nature of primary charge carriers (that is, n- or p-type). Magnetic susceptibility of the samples $NaCuMS_2$ (M = Mn, Fe, Co) was measured with a SQUID magnetometer (MPMS, Quantum Design) in an applied field of 0.1−0.5 T in the temperature range 2−300 K. The magnetic data was corrected, when appropriate, for the core-diamagnetism of the constituting atoms: $Na^+ = -5 \times 10^{-6}$ emu/mol, $Cu^+ = -12 \times 10^{-6}$ emu/mol, $S^{2-} = -38 \times 10^{-6}$ emu/mol, $Mn^{2+} = -14 \times 10^{-6}$ emu/mol, $Fe^{2+} = -13 \times 10^{-6}$ emu/mol, $Co^{2+} = -12 \times 10^{-6}$ emu/mol.[23]

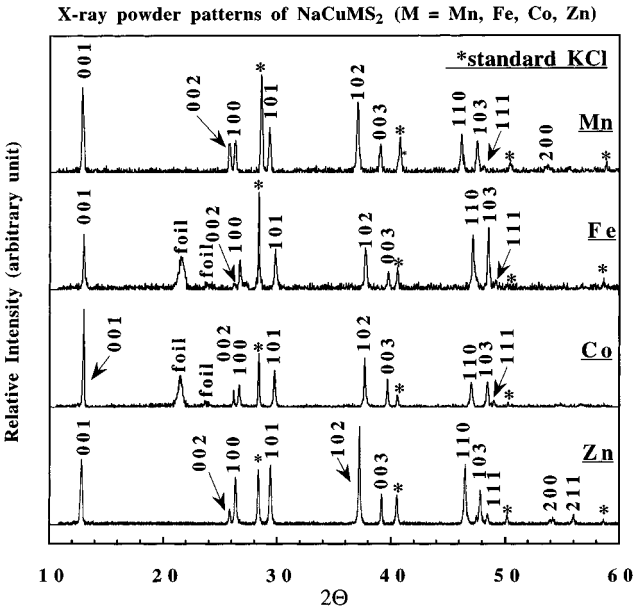

Figure 2. Powder X-ray diffraction pattern of the new quaternary sulfides $NaCuMS_2$ (M = Mn, Fe, Co, and Zn).

Table 1. Unit Cell Parameters and Room-Temperatures Resistivities of $NaCuMS_2$ (M = Mn, Fe, Co, and Zn) Phases, and Unit Cell Parameters of $NaCu_{1.5}V_{0.5}S_2$

composition	a (Å)	c (Å)	ρ(RT) (10^{-2} Ω·cm)
$NaCu_{1.5}V_{0.5}S_2$[a]	3.862(1)	6.822(1)	
$NaCuMnS_2$	3.9485(8)	6.959(2)	20
$NaCuFeS_2$	3.849(2)	6.808(3)	5.1
	3.873(1)[b]	6.848(4)[b]	
	3.863(1)[c]	6.873(1)[c]	
$NaCuCoS_2$	3.8645(4)	6.809(6)	5.5
$NaCuZnS_2$	3.9022(6)	6.894(1)	62

[a] Reference 24. [b] Mineral chvilevait (ref 6). [c] Reference 2.

Results and Discussion

All of the $NaCuMS_2$ (M = Mn, Fe, Co, Zn) compounds adopt the $CaAl_2Si_2$-type structure as evidenced from the similarity of their powder diffraction profiles presented in Figure 2. The patterns were indexed on the basis of a trigonal unit cell (space group $P\bar{3}m1$, #164). The lattice parameters, determined by the least-squares fitting of the d-spacings corrected for systematic errors, are presented in Table 1. The absence of superlattice reflections corresponding to a long-range order of transition metal ions indicates that these ions might be distributed randomly at the tetrahedral sites. However, to determine unambiguously the distribution of the transition metal ions, neutron diffraction data should be analyzed. X-ray powder diffraction data do not constitute a definite proof of cation order/disorder, for the differences in the atomic number between Cu and Mn, Fe, Co, and Zn are very small.

The unit cell parameters of all the phases are in general agreement with those reported for $NaCuFeS_2$ providing further evidence for the structural uniformity across the series. The discrepancy in the lattice pa-

(22) Llanos, J.; Tejeda, M.; Contreras-Ortega, C.; Mujica, C. *J. Chem. Soc., Chem. Commun.* **1991**, *96*, 1068.

(23) König, E *Magnetic Properties of Transition Metal Compounds*; Hellwege, K.-H., Hellwege, A. M., Eds.; Landolt-Börnstein, New Series, Group II, Springer-Verlag: Berlin, Heidelberg, New York; 1966; p 1.

Table 2. Results of the Elemental Analysis of $NaCuMS_2$ (M = Mn, Fe, Co, Zn) Phases

composition[a]	Na (wt %)	Cu (wt %)	M (wt %)	S (wt %)[b]
$NaCuMnS_2$				
observed	11.3	30.5	24.0	34.0
calculated	*11.2*	*30.9*	*26.7*	*31.2*
$NaCuFeS_2$				
observed	11.2	28.0	22.9	37.8
calculated	*11.1*	*30.8*	*27.0*	*31.2*
$NaCuCoS_2$				
observed	11.0	28.1	23.5	37.4
calculated	*11.0*	*30.3*	*28.1*	*30.6*
$NaCuZnS_2$				
observed	10.3	25.1	28.4	36.3
calculated	*10.6*	*29.4*	*30.3*	*29.7*

[a] All wt % are ±2 wt %. [b] Sulfur content determined by weight difference.

rameters of $NaCuFeS_2$ reported by various authors can be ascribed to deviations from the ideal composition. For example, the unit cell parameters reported by Katchalovskaya et al. refer to the mineral chvilevait with the composition Na(Cu, Fe, Zn)S_2 with trace amounts of Ca, As and Mn.[6] Similarly, the elemental analysis of $NaCuFeS_2$ reported by Llanos et al.[2] points to the deficiency of Na and Fe.

Semiquantitative electron microscope analyses, as well as SEM/EDS analyses, indicated the presence of the four elements in each sample. Due to interference of sodium and copper and sodium and zinc peaks, however, the content of sodium determined by both of these methods cannot be regarded as reliable. The DCP-AES method turned out to be more suitable and more accurate in this case, for the content of each metal was found from a corresponding calibration curve (Table 2). By visual inspection, SEM images of the samples' surface did not provide evidence for compositional inhomogeneity. On the other hand, DCP analyses, performed on bulk specimen, indicate an excess of sufur in all of the samples. Since in the DCP method the sulfur content is determined by weight difference, there is an anticorrelation between sulfur content and the sum of the contents of the other elements in each sample. Hence, an error associated with the sulfur content can be greater than that for a single element (±2%) and might contribute to the observed discrepancies between the calculated and the experimental values (Table 2).

In the series $NaCuMS_2$ we have not succeeded in the synthesis, employing similar experimental conditions, of the quaternary phases with M = Cr or Ni. We obtained the mixture of products containing $NaCrS_2$ and $Na_3Cu_4S_4$ in the former case, and NiS and $Na_3Cu_4S_4$ in the latter. Recently, Mujica et al. reported on the synthesis of another quaternary sulfide, $NaCu_{1.5}V_{0.5}S_2$, which crystallizes in the trigonal space group $P\bar{3}$.[24] This compound was prepared by a reaction between the mineral sulvanite, Cu_3VS_4, and Na_2S in sulfur atmosphere at 1173 K. Similar to the $NaCuFeS_2$ phase, the $NaCu_{1.5}V_{0.5}S_2$ compound is air and moisture sensitive. On the basis of Pauling electronegativities of the 3d transition metals (Table 3 [25,26]) in the $NaCuMS_2$ systems investigated in this study, it is difficult to reconcile the observed trend in the stabilities of the $NaCuMS_2$ phases with the well-established concept that by reducing the ionicity of the layer, its stability should increase (e.g., see ref 27). In this series the most stable compounds are those containing the less electronegative metals, that is, Mn and Zn. The factors that may account for the observed trend in the stabilities of the $NaCuMS_2$ phases may include, among others: (a) the relative stabilities of the M^{2+} and M^{3+} ions; (b) the occupancy of the 3*d* transition metal energy levels; (c) the size of the M^{2+} cation and its preference for tetrahedral coordination (Table 3); (d) the entropy factors associated with the presence of two types of transition metals randomly distributed over the tetrahedral sites. "$NaCuCrS_2$" does not form most likely because of the difficulty of stabilizing the Cr^{2+} ions in the tetrahedral site.

Table 3. Pauling Electronegativities and Ionic Radii of Selected 3d Transition Metals[a]

transition metal	electronegativity	$r_{M^{2+}(IV)}$ (Å)	transition metal	electronegativity	$r_{M^{2+}(IV)}$ (Å)
V	1.63		Co	1.88	0.72
Cr	1.66		Ni	1.91	0.69
Mn	1.55	0.80	Cu	1.90	0.71 (0.74)[b]
Fe	1.83	0.77	Zn	1.65	0.74

[a] After refs 25 and 26. [b] Radius of Cu^+(IV).

Physical Properties. *$NaCuMnS_2$.* Parts a and b of Figure 3 show the temperature variation of the resistivity (ρ) and the magnetic susceptibility (χ), respectively, for the $NaCuMnS_2$ compound. Although the positive temperature dependence of ρ is indicative of metallic behavior, the high value of room-temperature resistivity ρ_{RT} ($\sim 10^{-1}$ Ω·cm) is typical for a semiconductor, based on Mott's maximum metallic resistivity 10^{-2}–10^{-3} Ω·cm.[28] Therefore, assuming that grain boundary effects do not dominate the resistivity, $NaCuMnS_2$ should be considered a doped or a degenerate semiconductor, rather than a metal. A qualitative Seebeck measurement indicates that the primary charge carriers are holes. We observed similar ρ versus T behavior for the $ACuMnS_2$ (A = K, Rb, Cs) phases with $ThCr_2Si_2$-type structure.[14] In both systems, the transport properties are determined by the $CuMnS_2^-$ framework, which is made up either of single layers of edge-sharing (Cu, Mn)S_4 tetrahedra (as in the $ThCr_2Si_2$-type structure) or double layers of edge-sharing (Cu, Mn)S_4 tetrahedra (as in the $CaAl_2Si_2$-type structure). The magnetic susceptibility of $NaCuMnS_2$ as a function of temperature, however, differs markedly from that observed for $ACuMnS_2$ phases with the $ThCr_2Si_2$-type structure. The latter exhibit short-range antiferromagnetic interactions at higher temperatures (100–300 K) and a spin-glass-like behavior below 100 K.[14] The temperature dependence of χ for $NaCuMnS_2$ suggests the presence of localized magnetic moments. The magnetic susceptibility of the $NaCuMnS_2$ sample (Figure 3b) was fitted to a modified Curie–Weiss law: $\chi = \chi_0 + C/(T - \theta)$, where χ_0 represents temperature-independent contributions such as van Vleck and Pauli paramagnetic susceptibili-

(24) Mujica, C.; Llanos, J.; Carvajal, G.; Wittke, O. *Eur. J. Solid State Inorg. Chem.* **1996**, *33*, 987.
(25) Cotton, F. A.; Wilkinson, G. *Advanced Inorganic Chemistry*; John Wiley & Sons: New York,1988.
(26) Shannon, R. D. *Acta Crystallogr.* **1976**, *A32*, 751.
(27) Rouxel, J.; Tournoux, M. *Solid State Ionics* **1996**, *84*, 141.
(28) Cheetham, A. K.; Mahesh, R. *Chem. Mater.* **1996**, *8*, 2421.

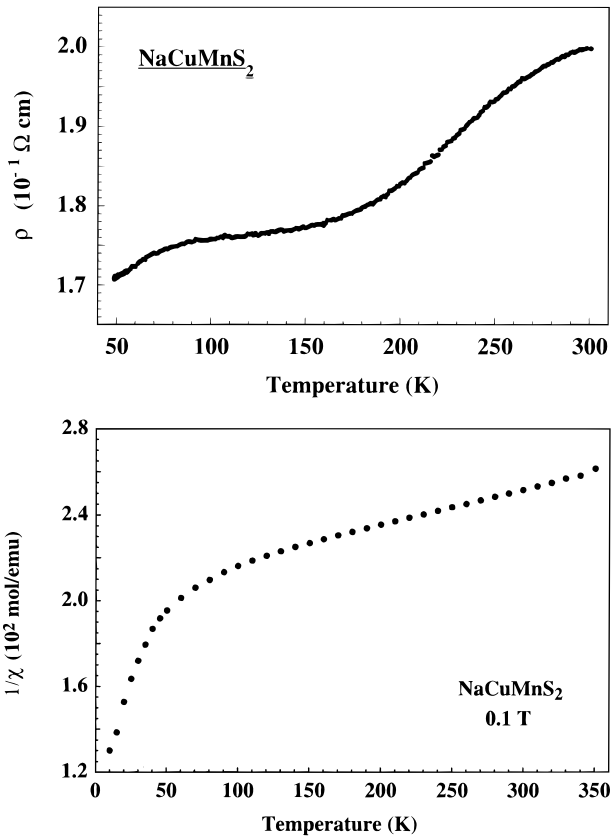

Figure 3. (a) Resistivity (ρ) as a function of temperature for $NaCuMnS_2$. (b) Inverse magnetic susceptibility (χ) as a function of temperature for $NaCuMnS_2$.

ties, C is the Curie constant, and θ is the Weiss constant. A nonlinear least-squares analysis in the temperature range 120−350 K yielded, $\chi_0 = 5.0 \times 10^{-4}$ emu/mol, $\theta \approx -10^3$ K, and the effective magnetic moment, $\mu_{eff} = 5.98\ \mu_B$. The observed μ_{eff} is in good agreement with that expected for high-spin Mn^{2+} ion ($5.92\ \mu_B$) assuming spin-only contributions. The observed magnetic moment of $NaCuMnS_2$ solely corresponds to the Mn^{2+} centers in the structure, since sodium carries no unpaired electrons and copper in sulfides is considered to be monovalent and diamagnetic (e.g., see ref 16). Although no long-range magnetic order is evident in this composition, the large negative value of the Weiss constant implies strong antiferromagnetic exchange correlations between the Mn^{2+} centers.

$NaCuFeS_2$. The temperature dependence of ρ for $NaCuFeS_2$ is presented in Figure 4a. The decrease of ρ with decreasing temperature is suggestive of metallic behavior. Although the value of ρ for $NaCuFeS_2$ (10^{-2} Ω·cm) is approximately an order of magnitude smaller than that of the $NaCuMnS_2$ phase, it barely satisfies Mott's criterion of maximum metallic resistivity. Therefore, the $NaCuFeS_2$ phase should also be classified as a highly doped or a degenerate semiconductor, rather than a metal. A qualitative Seebeck measurement indicates that the conductivity is n-type. The observed electrical properties of the $NaCuFeS_2$ phase are very similar to those reported for the chalcopyrite, $CuFeS_2$. According to the published reports, chalcopyrite is a degenerate semiconductor, with the conductivity value on the borderline between metallic and semiconducting regimes ($10^3\ \Omega^{-1}\cdot cm^{-1}$ at 100 K). The temperature

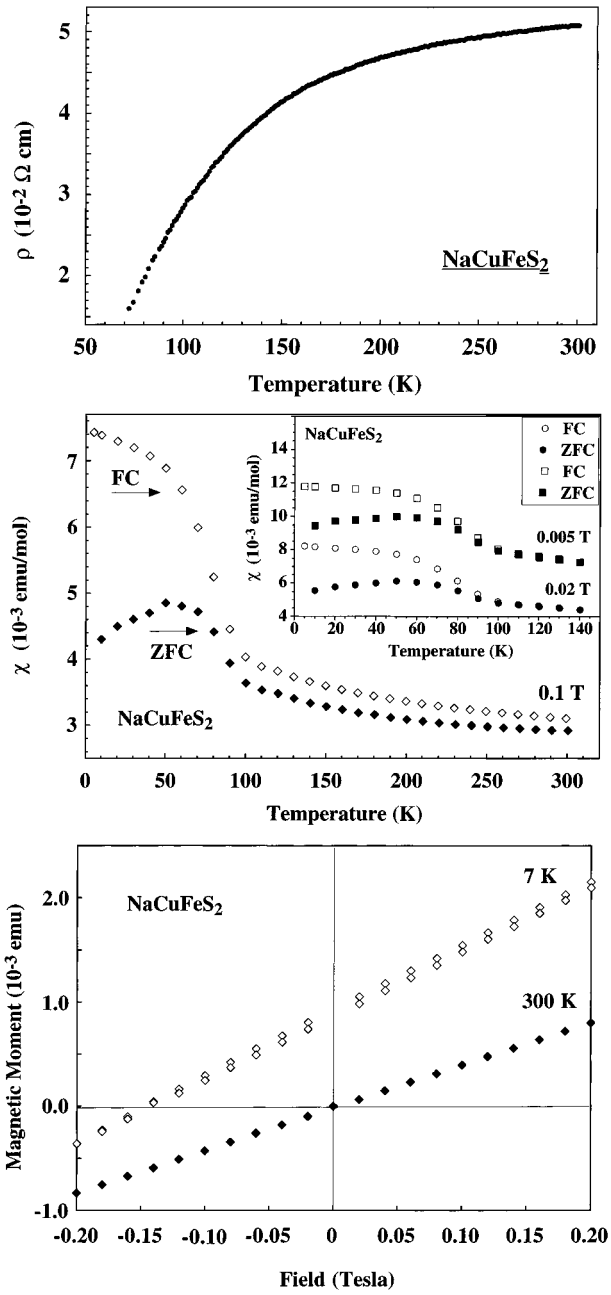

Figure 4. (a) Resistivity (ρ) as a function of temperature for $NaCuFeS_2$. (b) Inverse magnetic susceptibility (χ) as a function of temperature for $NaCuFeS_2$. (c) Magnetic moment as a function of magnetic field for $NaCuFeS_2$.

dependence of ρ and that of the carrier concentration, however, are consistent with metallic behavior.[29] Moreover, the conductivity of the chalcopyrite is also n-type.[30] Upon the insertion of a stoichiometric amount of sodium ions into the chalcopyrite, the copper ions remain monovalent, whereas the Fe^{3+} ions are reduced to Fe^{2+}.[31] The observed higher ρ of $NaCuFeS_2$ relative to $CuFeS_2$ is therefore expected, since the band associated with Fe^{2+} most probably will lie higher in energy than that associated with Fe^{3+}, thereby reducing the width

(29) Teranishi, T. *J. Phys. Soc. Jpn.* **1961**, *16*, 1881.
(30) Kradinova, L. V.; Polubotko, A M.; Popov, V. V.; Prochukhan, V. D.; Rud, Y. V.; Skoriukin, V. E. *Semicond. Sci. Technol.* **1993**, *8*, 1616.
(31) Llanos, J.; Buljan, A.; Mujica, C. *Mater. Res. Bull.* **1995**, *30*, 43.

of the conduction bands. The electronic band structure calculations of Ramírez et al. for $ACuFeS_2$ (A = Li and Na) indicate a relatively small density of states near the Fermi level consistent with the observed high resistivities.[11] Badwal et al.[32] reported that $Li_{1.33}Cu_{0.67}FeS_2$, with the $CaAl_2Si_2$-type structure, is a semiconductor. The room-temperature resistivity, ρ(RT), of $Li_{1.33}Cu_{0.67}FeS_2$ is $\sim 6 \times 10^{-2}$ Ω·cm and is similar to that of $NaCuFeS_2$ ($\sim 5 \times 10^{-2}$ Ω·cm). In contrast to what we observed in the $ACuMnS_2$ (A = Na, K, Rb, Cs) series, the electrical properties of $NaCuFeS_2$ do not resemble those of the $ACuFeS_2$ (A = K, Rb, Cs) phases with $ThCr_2Si_2$-type structure. All of the $ACuFeS_2$ (A = K, Rb, Cs) phases are thermally activated semiconductors [ρ(RT) $\approx 10^2$ Ω·cm], with the ρ value being too high below 200 K to be detected with our setup.[12] We believe that this contrasting behavior can be partly attributed to the structure of the $NaCuFeS_2$ phase, in which the double layers of edge-sharing tetrahedra resemble more the three-dimensional framework of the chalcopyrite than the $ThCr_2Si_2$-type structure with single layers of edge-sharing tetrahedra.

The variation of the magnetic susceptibility of $NaCuFeS_2$ with temperature is shown in Figure 4b. The nearly temperature-independent susceptibility observed in the high-temperature region is consistent with its low-resistivity and semiconducting behavior and more importantly reveals that there are no localized magnetic moments associated with the Fe^{2+} ions. As discussed earlier, in the case of $NaCuFeS_2$, the electronic band structure calculations support the formation of oligomeric cluster units comprising Fe−Fe bonds.[11] Thus, it is reasonable to assume that the $3d^6$ electrons of iron are partly utilized for the metal−metal bonds or are mostly delocalized, thereby accounting for the absence of localized moments. However, the cusp seen in the susceptibility at ~50 K appears to be related to a spin-glass-like transition, as evidenced by the divergence of the of zero-field-cooled (ZFC) and field-cooled (FC) data. To further confirm that the feature in the ZFC data at ~50 K in Figure 4b corresponds indeed to the onset of a transition to a spin-glass state, additional ZFC and FC data were collected at 5 and 20 mT, respectively. The expected divergence of ZFC and FC data was observed at both these fields; however, the variation of the spin-freezing temperature as a function of field could not be precisely estimated, because of the broad shape of the cusp. The spin-glass-like behavior suggested by the ZFC/FC irreversibilty was subsequently confirmed by measuring the field-cooled hysteresis data at 7 and 300 K (Figure 4c). The room-temperature loop shows no hysteresis and passes through the origin as expected for a normal paramagnet, whereas the 7 K data shows hysteresis with the resulting loop being displaced from the origin. Such a displacement can be taken as evidence for spin-glass behavior.[33] In case of a weak ferromagnetism the hysteresis loop would be symmetric about the origin. Nevertheless, unambiguous confirmation of the collective freezing of the magnetic spins must be made by frequency- and field-dependent ac susceptibility measurements.

(32) Badwal, S. P. S.; Thorn, R. J. *J. Solid State Chem.* **1982**, *43*, 163.

(33) Ford, P. J. *Contemp. Phys.* **1982**, *23*, 141.

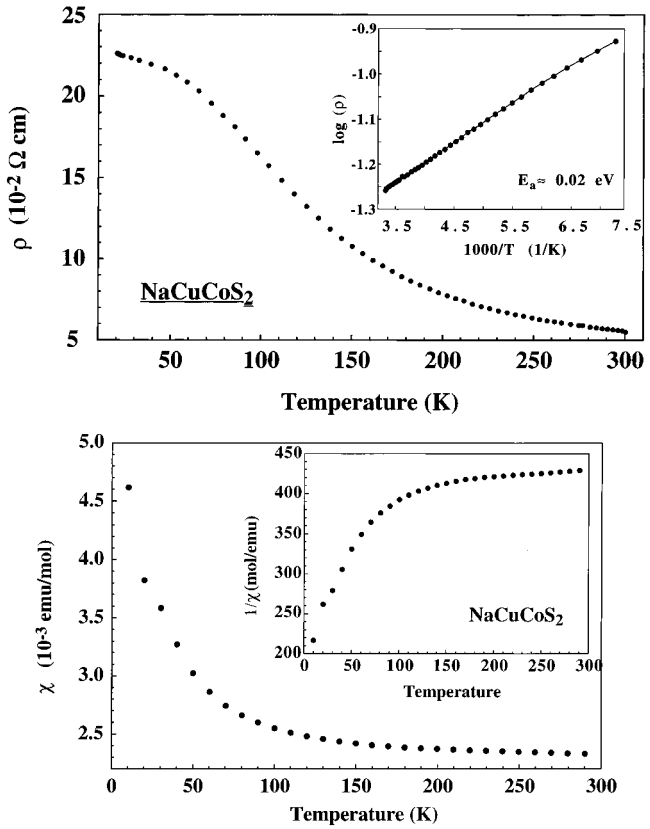

Figure 5. (a) Resistivity (ρ) as a function of temperature for $NaCuCoS_2$. Inset shows log(ρ) vs 1000/T. (b) Magnetic susceptibility (χ) as a function of temperature for $NaCuCoS_2$. Inset shows 1/χ vs T.

$NaCuCoS_2$. Electrical resistivity as a function of temperature reveals that ρ increases exponentially with decreasing temperature, indicating semiconducting behavior (Figure 5a). The thermal activation energy for conduction (E_a) estimated from the linear portion of the plot of log ρ vs 1000/T (the inset of Figure 5a) is 0.02(1) eV, in the temperature range 140−300 K. The primary charge carriers are holes, as evidenced by Seebeck measurement. The electrical properties of the $NaCuCoS_2$ phase closely resemble those of the $ACuCoS_2$ (A = K, Rb, Cs) phases with $ThCr_2Si_2$-type structure, which are also p-type degenerate semiconductors with similar values of ρ (300 K) and $E_a \approx 0.02$ eV.[13] The magnetic behavior of the $NaCuCoS_2$ phase, however, differs significantly from that observed for the $ACuCoS_2$ (A = K, Rb, Cs) phases with $ThCr_2Si_2$-type structure. The $ACuCoS_2$ (A = K, Rb, Cs) series exhibit complex magnetic behavior due to anisotropic magnetic interactions: ferromagnetic in the *ab* plane and antiferromagnetic along the *c*-axis. In contrast, the magnetic susceptibility of the $NaCuCoS_2$ compound remains nearly temperature-independent over the temperature region $100 < T < 300$ K (Figure 5b). This behavior, indicative of delocalized or partially delocalized electrons, correlates well with the observed low resistivity. The low-temperature upturn seen in the χ vs T plot at temperatures below ~100 K indicates a small concentration of paramagnetic impurities.

$NaCuZnS_2$. Parts a and b of Figure 6 show variable-temperature ρ and variable-temperature χ, respectively. The observed increase in the electrical resisitivity with decreasing temperature as well as the relatively high

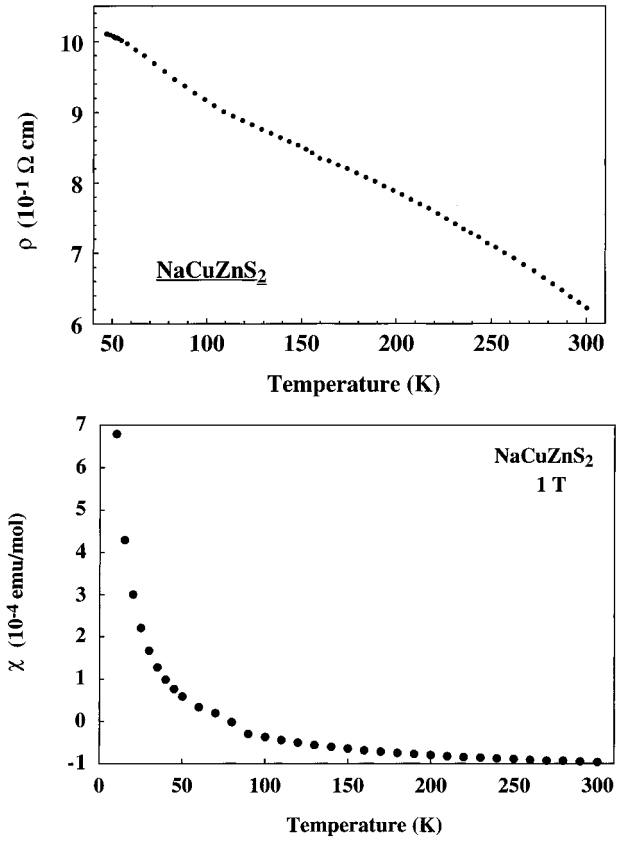

Figure 6. (a) Resistivity (ρ) as a function of temperature for $NaCuZnS_2$. (b) Magnetic susceptibility (χ) as a function of temperature for $NaCuZnS_2$.

room-temperature resistivity ρ ($\sim$1Ω·cm) indicate that the compound is a semiconductor. The primary charge carriers are electrons, as evidenced by a qualitative Seebeck measurement. The small negative values of χ at room temperature are representative of diamagnetism. The diamagnetism observed in this phase is consistent with the filled-shell electronic configurations of the metal ions. The paramagnetic impurity contributions increases the overall value of χ at low temperatures. The semiconducting and diamagnetic properties of the $NaCuZnS_2$ phase resemble those of the zinc blende ZnS. The latter was reported to be either a n- or p-type semiconductor, although it is generally regarded as n-type, because p-type ZnS cannot be prepared.[34]

Conclusions

We have prepared four new quaternary low-dimensional sulfides, $NaCuMS_2$, M = Mn, Fe, Co, and Zn, and investigated their structure, electrical and magnetic properties. All the compounds crystallize with the well-known $CaAl_2Si_2$-type structure. The stability of quaternary sulfides, presented in this study, seems to be governed by factors other than electronegativity considerations of the metal-sulfur network. All phases, except for M = Zn, are small-bandgap semiconductors with their normal state electrical resistivities higher than that required to satisfy Mott's criterion of metallicity. The $NaCuZnS_2$ phase is a diamagnetic insulator. Magnetization studies revealed the presence of localized moments for M = Mn and a spin-glass-like behavior for M = Fe at $\sim$ 50 K. The transport properties of $NaCuFeS_2$ reported in this study appear to correlate well with the recently proposed electronic band structure of the $[CuFeS_2]^-$ layers.

Acknowledgment. We thank Dr. Lina Patino for the DCP-AES measurements, Dr. R. McCauley for the SEM/EDS data, and Dr. J. S. Delaney for the microprobe analyses and helpful discussions. One of us (K.V.R.) would like to thank Rowan University for the award of a Separately Budgeted Research grant and release time. This work was supported by the National Science Foundation, Solid State Chemistry Grants DMR-93-14605 and DMR-96-13106.

CM9704793

(34) Wold, A.; K. Dwight, K. *Solid State Chemistry: Synthesis, Structure and Properties of Selected Oxides and Sulfides*; Chapman & Hall: New York, 1993; p 200.